Direct observation of the pressure-induced charge redistribution in $BiNiO_3$ by x-ray absorption spectroscopy

Masaichiro Mizumaki,[1,*] Naoki Ishimatsu,[2] Naomi Kawamura,[1] Masaki Azuma,[3] Yuichi Shimakawa,[3] Mikio Takano,[3] and Takayuki Uozumi[4]

[1]*Japan Synchrotron Radiation Research Institute, SPring-8, 1-1-1 Kouto, Sayo-cho, Sayo-gun, Hyogo 679-5198, Japan*

[2]*Department of Physical Sciences, Graduate School of Science, Hiroshima University, 1-3-1 Kagamiyama, Higashi-Hiroshima, Hiroshima 739-8526, Japan*

[3]*Institute for Chemical Research, Kyoto University, Uji, Kyoto 611-0011, Japan*

[4]*Osaka Prefecture University, 1-1 Gakuen-cho, Sakai, Osaka 599-8531, Japan*

(Received 2 April 2009; revised manuscript received 23 November 2009; published 28 December 2009)

To investigate the change in the electronic structure of $BiNiO_3$ accompanied by metal-insulator (MI) transition, we measured x-ray absorption spectroscopy (XAS) spectra at the Ni *K* and Bi *L* edges under various pressures up to 6 GPa. Both Bi L_3 and Ni *K* edge XAS spectra clearly change at 4 GPa, indicating the electronic state in Bi and Ni ion changes. A quantitative analysis of the Ni *K* edge spectra in the pre-edge region based on the charge-transfer cluster model including multiplet terms revealed that the electronic configuration changes from d^8 in the insulating phase to 56% d^7+44% $d^8\underline{L}$ in the metal phase. From these results, we concluded that the MI transition in $BiNiO_3$ is induced by the collapse of charge-transfer gap and is governed by the redistribution of O 2*p* ligand holes.

DOI: 10.1103/PhysRevB.80.233104 PACS number(s): 71.30.+h, 74.62.Fj, 78.70.Dm

Perovskite oxides show various interesting physical properties such as colossal magnetoresistance, superconductivity, ferroelectricity, ferromagnetism and antiferromagnetism, and metal-insulator (MI) transition. RNiO$_3$ (R=earth and Lu-Pr) exhibits an MI transition as a function of R-ion radius and temperature in a systematic manner.[1–5] The MI transition of RNiO$_3$ is due to the charge disproportionation expressed as $2Ni^{3+} \rightarrow Ni^{(3+\delta)} + Ni^{(3-\delta)}$ associated with the reduction in crystallographic symmetry from orthorhombic *Pbmn* to monoclinic $P2_1/n$. The transition temperature T_{MI} decreases with increasing R-ion radius and the least distorted $LaNiO_3$ remains as a rhombohedral paramagnetic metal down to the lowest temperature.[6] In this context, the replacement of La^{3+} with a larger ion, such as Bi^{3+}, might be expected to lead to a better metallicity in the cubic perovskite structure. However, $BiNiO_3$ does not follow this trend and has proven to be a seriously distorted antiferromagnetic insulator with localized spins of $S=1$.[7] This fact suggests that the origin of the insulating nature of $BiNiO_3$ is different from that of RNiO$_3$.[8] Indeed, structural analyses by synchrotron x-ray and neutron diffractions revealed that the valence state of $BiNiO_3$ is $Bi^{3+}_{0.5}Bi^{5+}_{0.5}Ni^{2+}O_3$.[7,9] The insulating nature of this compound is due to the divalent Ni ion. It should be learned here that the Bi ions are not an inert presence as La ions but play an important role in the electronic properties: in other words, this oxide is not a simple Ni 3*d*–O 2*p* system but is a Bi 6*s*–Ni 3*d*–O 2*p* electronic system. $BiNiO_3$ shows MI transitions by La substitution for Bi or the application of a high pressure of 4 GPa.[10] Core-level x-ray photoemission spectroscopy (XPS) and x-ray absorption measurement around the Ni *L* edges revealed that the average Bi valence of 4+ is stable to the La substitution and that the hole doping to the Ni^{2+} ion leads to metallization.[8] Recently, Azuma *et al.* proposed that the pressure-induced MI transition is caused by the melting of Bi-charge disproportionation and simultaneous Ni→Bi charge transfer: $Bi^{3+}_{0.5}Bi^{5+}_{0.5}Ni^{2+}O_3 \rightarrow Bi^{3+}Ni^{3+}O_3$.[11] However, this integer valence model is too simple to describe the actual electronic states in $BiNiO_3$. Hard x-ray absorption spectroscopy (XAS) is a powerful tool for studying the electronic state changes under pressure because the high-energy x-ray easily transmits the diamond anvil cell. In this Brief Report, we report the direct measurement of the valence states of Bi and Ni ions by XAS around the Bi *L* (L_1 and L_3) and Ni *K* edges, which are sensitive to the valence state, the hybridization between Bi 6*p*, −6*s*, −5*d*, Ni 3*d*, and O 2*p* states, and local environment of an absorption ion, under various pressures. Using the obtained XAS spectra, we explain the mechanism of the pressure-induced MI transition of $BiNiO_3$.

Polycrystalline $BiNiO_3$ was prepared at 6 GPa and 1000 °C with a cubic anvil-type high pressure apparatus, as reported in Ref. 7. The XAS measurements at the Bi $L_{1,3}$ and Ni *K* edges under various pressures were carried out by synchrotron radiation at the beamline BL39XU of SPring-8, Japan.[12] The energy resolution $\Delta E/E$ is smaller than 1×10^{-4} around the Bi $L_{1,3}$ and Ni *K* edges. Incident and transmitted x-ray intensities were monitored using ionization chambers before and after the sample. All the measurements were performed at room temperature. A diamond anvil cell (DAC), which is an assembled pair of diamond anvils with a culet diameter of 0.6 mm, was used to apply the pressure up to 6 GPa. A powdered sample and a mixture of $CH_3OH:C_2H_5OH=4:1$ as a pressure medium were sealed inside the DAC. The pressure inside the DAC was determined by measuring the wavelength of ruby fluorescence.

Figures 1(a) and 1(b) show the XAS spectra around the Bi L_1 ($2s\rightarrow6p$) and L_3 ($2p\rightarrow6d$ and $6s$) edges. The data collected at 5.8 GPa correspond to the metallic (M) phase, while the ambient pressure (AP) and 2.8 GPa data represent the insulating (I) phase. The Bi L_1 XAS spectra show single-peak structures. No notable difference was observed between the M and I phases, reflecting the same empty 6*p* states in

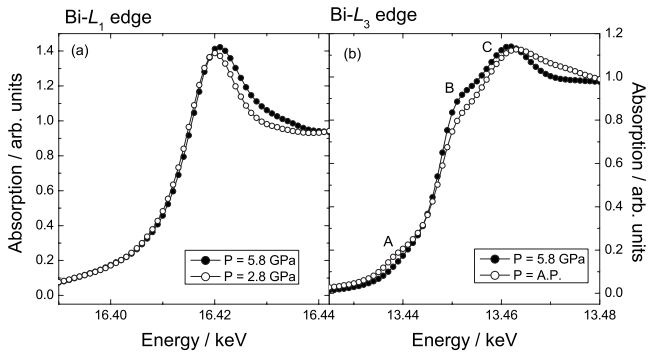

FIG. 1. (a) XAS spectra around Bi L_1 XAS spectra for $BiNiO_3$ at $P=5.8$ GPa (closed circles) and 2.8 GPa (open circles). (b) XAS spectra around Bi L_3 XAS spectra for $BiNiO_3$ at $P=5.8$ GPa (closed circles) and ambient pressure (open circles).

Bi^{3+} and Bi^{5+} ions. On the other hand, the Bi L_3 XAS spectra at 5.8 GPa and AP changed significantly. These are composed of three peaks (labeled A, B, and C) near the absorption edge. The change in the energy region higher than peak C is due to the triclinic-to-orthorhombic structural transition because the extended x-ray absorption fine structure (EXAFS) region mainly reflects the local structure of absorbing atoms. Another difference is the absence and presence of peak A.[10] From the comparison with the spectra of $BaBiO_3$ and its related compounds,[13] this peak is assigned to the $2p \rightarrow 6s$ transition. The absence of peak A therefore indicates a filled Bi $6s$ state. The present result indicates the valence change of Bi from 3+ in the M phase to a higher value in the I phase. The first-principles band calculation also shows that the number of unoccupied Bi $6s$ states in the I phase is larger than that in the M phase. It should be noted that the Bi $6s$ band above 0.7 eV from Fermi energy strongly hybridized with O $2p$ states in the I phase.[11] This implies the possibility that the electronic state of Bi^{3+} is not simple formal valence of trivalent but Bi $6s$ and O $2p$ states strongly hybridized.

Figure 2 shows the XAS spectra around the Ni K edge of the metallic (6.0 GPa) and insulating (2.5 GPa) phases for $BiNiO_3$ and metallic $PrNiO_3$ as a trivalent nickel reference. Three differences were found between the M and I phases, i.e., the spectral shape change in the energy region higher than 8.36 keV, the absorption edge energy (E_0^K) shift, and the intensity change in the pre-edge region. The first change is due to the triclinic-to-orthorhombic structure phase transition induced by pressure because this energy region is located in the EXAFS region. E_0^K is a good measure of the Ni valence change. The observed E_0^K shift from 8.3503 keV in the M phase to 8.3495 keV in the I phase indicates the decrease in Ni valence. This result supports the Ni valence changes from 3+ to 2+ as estimated by crystal structure analysis. The reason why the E_0^K of the M phase is lower than that of $PrNiO_3$ will be discussed later. Figure 3 shows the pressure dependence of E_0^K as determined from the second derivative of the observed XAS spectra. Open and closed circles represent the data collected on increasing and decreasing the pressure, respectively. The energy shift is estimated to be about 1 eV. The data show a hysteresis of about 1 GPa. This behavior coincides with the electric resistivity change, as shown in the

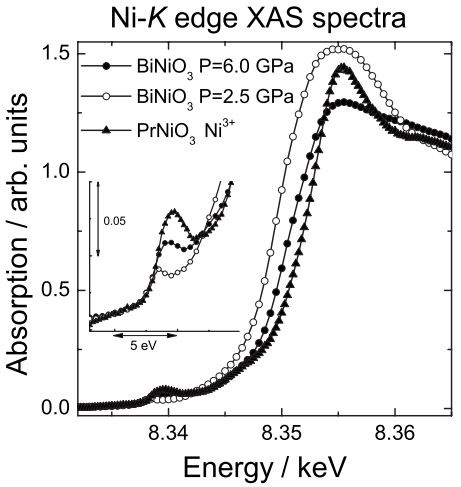

FIG. 2. Ni K edge XAS spectra for $BiNiO_3$ at $P=6.0$ GPa (closed circles) and 2.5 GPa (open circles) and for $PrNiO_3$ (closed triangles) which is a typical sample contained Ni^{3+} ions. Inset: Ni K pre-edge XAS spectra for $BiNiO_3$ at $P=6.0$ GPa (closed circles) and 2.5 GPa (open circles) and for $PrNiO_3$ (closed triangles) which is a typical sample containing Ni^{3+} ions.

inset of Fig. 3. This strongly suggests that the electronic state change of Ni is the origin of the pressure-induced I-to-M transition.

The pre-edge region reflects the Ni $3d$ electronic state because the $1s \rightarrow 3d$ electric quadrupole transition is dominant. As shown in the inset of Fig. 2, the absorption intensity in the pre-edge region is higher in the M phase. This also indicates the change in Ni valence. To quantitatively investigate the changes in Ni $3d$ electronic states in the M and I phases, we compared the observed XAS spectra with calculation results. The NiO_6 cluster model including the full-multiplet effects in a Ni ion was employed to describe the Ni $3d$ states and O $2p$ ligand states of $BiNiO_3$.

The Hamiltonian for the present model is given by

$$H = H_{\mathrm{Ni}} + H_{\mathrm{O}} + H_{\mathrm{Ni\text{-}O}}, \tag{1}$$

where the terms describe the following interactions: H_{Ni} includes the Ni $3d$ level ε_d, the crystal-field splitting of 10 Dq,

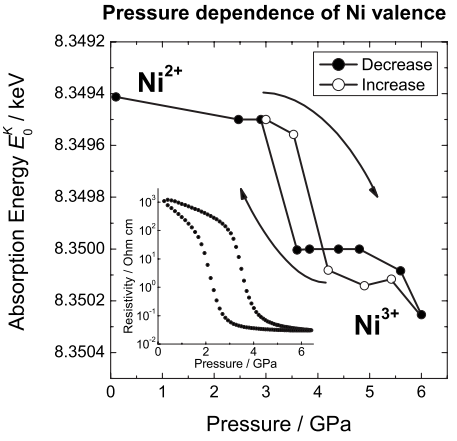

FIG. 3. Pressure dependence of absorption energy around Ni K XAS spectra for $BiNiO_3$. Inset: pressure dependence of electric resistivity of $BiNiO_3$ at room temperature.

TABLE I. Parameter values used in our calculations.

Parameter (unit: eV)	Δ	10 Dq	U_{dd}	U_{dc}	$V(e_g)$
Insulating phase	4.0	1.5	6.5	8.0	1.8
Metallic phase	−1.0	1.5	6.5	8.0	2.3

the $3d$ Coulomb repulsive energy U_{dd}, and the $1s$ core-hole potential U_{dc} in addition to the full-multiplet interactions composed of the spin-orbit interaction for Ni $3d$ states and the multipole parts of $3d$-$3d$ and $3d$-$1s$ Coulomb interactions. H_O describes the O $2p$ level ε_p and $H_{Ni\text{-}O}$ describes the Ni $3d$–O $2p$ hybridization, which is given in terms of transfer integrals $(pd\sigma)$ and $(pd\pi)$. The transfer integrals are connected with the hybridization energies as follows:

$$V(t_{2g}) = \sqrt{3}pd\sigma,$$

$$V(e_g) = 2pd\pi. \quad (2)$$

The local symmetry around the Ni ion is approximated as octahedron (O_h).[14–16] It should be noted that the difference in the Ni-O bond lengths is less than 10% and the lowering of the symmetry to D_{4h} does not affect the result of the calculation.

The wave function of the ground state $(|g\rangle)$ is described by a linear combination of the d^n and $d^{n+1}\underline{L}$ electron configurations $(|g\rangle = c_n|d^n\rangle + c_{n+1}|d^{n+1}\underline{L}\rangle$, where c_n and c_{n+1} are coefficients), where $\underline{L}$ denotes a ligand (O $2p$) hole, i.e., starting from the configuration in nominal valence Ni^{3+} (Ni^{2+}) and filled (empty) oxygen ligands for the M phase (I phase). We adopted $n=7$ for the M phase and $n=8$ for the I phase. The $1s \rightarrow 3d$ electric quadrupole transition was considered in the calculation of the optical transition. The parameters used in the calculation are shown in Table I. In this calculation, the XAS spectra, which are calculated from the Fermi golden rule, are obtained with a Lorentzian function with width of 0.5 eV (half width at half maximum). The values determined by core-level XPS were adopted in the calculation of the I phase[8] and the values in the M phase were chosen in order to reproduce the experimental XAS spectra. Figures 4(a) and 4(b) show the observed (circles) and calculated (thick line) XAS spectra around the pre-edge region in the M and I phases, respectively. The calculated XAS spectra composed of the electric quadrupole contribution (shown with vertical bars), background originated from a low energy tail of the Ni $4p$ states (dipole contribution), and the absorption of the elements except Ni in the region below pre-edge (thin line). The calculated spectra excellently reproduced the experimental results for both the M and I phases. In the I phase, the Ni $3d$ electron number was estimated to be 8.11, which is close to the ideal value of 8 for a divalent Ni ion. The Ni $3d$ magnetic moment of $2.05\mu_B$ was also estimated by the analysis of the experimental XAS spectra.[17] This value is consistent with the ordered magnetic moment determined by neutron diffraction.[9] On the other hand, the Ni $3d$ electron number and the magnetic moment estimated for the M phase were 7.44 and $1.50\mu_B$, respectively. These indicate that the actual electronic configuration of the Ni^{3+} ion in the M phase

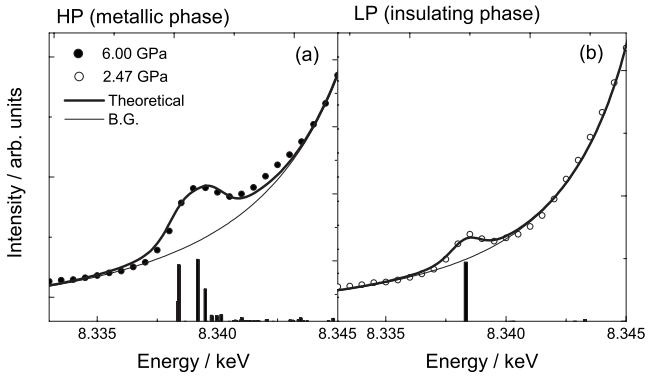

FIG. 4. Theoretical and experimental Ni K XAS spectra at (a) metallic and (b) insulating phases for $BiNiO_3$ around pre-edge region.

is $56(\pm5)\%d^7 + 44(\pm5)\%d^8\underline{L}$. It is interesting to compare these fractions with the electronic configuration for $PrNiO_3$, $32(\pm5)\%d^7 + 68(\pm5)\%d^8\underline{L}$, which were estimated in our model calculations using parameters reported previously.[18] The d^7-$d^8\underline{L}$ fraction changed depending on the A site of the Ni perovskite. This explains the difference of the absorption edge energy for the M phase and $PrNiO_3$. The large fraction is attributed to the slight shift of E_0^K to the lower energy with respect to E_0^K for $PrNiO_3$.

The effective Coulomb energy (U_{eff}) and effective charge-transfer energy (Δ_{eff}) including the multiplet effects are estimated to be $U_{eff}=7.8$ eV (6.0 eV) and $\Delta_{eff}=6.2$ eV (−0.12 eV) in the I (M) phase. The U_{eff} and Δ_{eff} are defined with respect to the lowest multiplet term energies as

$$U_{eff} = U_{dd} + 2\delta E(d^n) - \delta E(d^{n+1}) - \delta E(d^n\underline{L}) \quad (3)$$

and

$$\Delta_{eff} = \Delta + 2\delta E(d^n) - \delta E(d^{n+1}) - \delta E(d^{n-1}), \quad (4)$$

where $\delta E(d^n)$ denotes the energy difference between the configuration averaged energy and the lowest multiplet term energy of the d^n configuration.[19] Judging from these parameters, the I and the M phases were classified as the charge-transfer-type insulator and p-type metal phases in the Zannen-Sawatzky-Allen phase diagram, respectively.[20] This indicates that the I-to-M transition in $BiNiO_3$ originates from the collapse of the charge-transfer (Δ_{eff}) gap by pressure. In addition, the first-principles band calculation shows that the hybridization between Ni $3d$ and O $2p$ electrons is stronger (weaker) than that between Bi $6s$ and O $2p$ electrons near the Fermi energy in the M (I) phase.[11] These results indicate that the hole in O $2p$ plays an important role in the I-to-M transition, in other words, the O $2p$ ligand holes redistribute from Bi ions to Ni ions.[10]

In summary, we measured x-ray absorption spectra at Ni K and Bi $L_{1,3}$ edges under various pressures up to 6 GPa and investigated the change of the electronic state of $BiNiO_3$ accompanied with the MI transition. Both Bi L_3 and Ni K edge XAS spectra clearly change at 4 GPa, indicating the electronic state change in both ions. A quantitative analysis of Ni K pre-edge spectra with the aid of charge-transfer multiplet calculations revealed a Ni electronic configuration

change from d^8 to $56(\pm 5)\%d^7+44(\pm 5)\%d^8\underline{L}$ in $BiNiO_3$. We concluded that the I-to-M transition in $BiNiO_3$ is induced by the collapse of charge-transfer gap and the redistribution of O $2p$ ligand holes.

This work was partially supported by a Grant-in-Aid for Scientific Research from the Ministry of Education, Science, Sports and Culture (Grants No. 171105002, No. 18350097, No. 19GS0207, No. 19014010, No. 19340098, and No. 19052008), by the Global COE Program, "International Center for Integrated Research and Advanced Education in Materials Science," and by the Joint Project of Chemical Synthesis Core Research Institute and Elements Science and Technology Project. The XAS measurements were performed at the facilities of BL39XU (Proposal No. 2007A1511) in SPring-8 with the approval of the Japan Synchrotron Radiation Research Institute (JASRI).

*FAX: 81-791-58-2752; mizumaki@spring8.or.jp

[1] M. Imada, A. Fujimori, and Y. Tokura, Rev. Mod. Phys. **70**, 1039 (1998).
[2] P. Lacorre, J. B. Torrance, J. Pannetier, A. I. Nazzal, P. W. Wang, and T. C. Huang, J. Solid State Chem. **91**, 225 (1991).
[3] J. B. Torrance, P. Lacorre, A. I. Nazzal, E. J. Ansaldo, and C. Niedermayer, Phys. Rev. B **45**, 8209 (1992).
[4] M. L. Medarde, J. Phys.: Condens. Matter **9**, 1679 (1997).
[5] S. J. Kim, G. Demazeau, J. A. Alonso, and J. H. Choy, J. Mater. Chem. **11**, 487 (2001).
[6] J. L. García-Muñoz, J. Rodríguez-Carvajal, P. Lacorre, and J. B. Torrance, Phys. Rev. B **46**, 4414 (1992).
[7] S. Ishiwata, M. Azuma, M. Takano, E. Nishibori, M. Takata, M. Sakata, and K. Kato, J. Mater. Chem. **12**, 3733 (2002).
[8] H. Wadati, M. Takizawa, T. T. Tran, K. Tanaka, T. Mizokawa, A. Fujimori, A. Chikamatsu, H. Kumigashira, M. Oshima, S. Ishiwata, M. Azuma, and M. Takano, Phys. Rev. B **72**, 155103 (2005).
[9] S. J. E. Carlsson, M. Azuma, Y. Shimakawa, M. Takano, A. Hewat, and J. P. Attfield, J. Solid State Chem. **181**, 611 (2008).
[10] S. Ishiwata, M. Azuma, M. Hanawa, Y. Moritomo, Y. Ohishi, K. Kato, M. Takata, E. Nishibori, M. Sakata, I. Terasaki, and M. Takano, Phys. Rev. B **72**, 045104 (2005).
[11] M. Azuma, S. Carlsson, J. Rodgers, M. G. Tucker, M. Tsujimoto, S. Ishiwata, S. Isoda, and Y. Shimakawa, J. Am. Chem. Soc. **76**, 960 (2007).
[12] N. Kawamura, N. Ishimatsu, and H. Maruyama (unpublished).
[13] S. M. Heald, D. DiMarzio, M. Croft, M. S. Hegde, S. Li, and M. Greenblatt, Phys. Rev. B **40**, 8828 (1989).
[14] K. Okada, A. Kotani, and B. T. Thole, J. Electron Spectrosc. Relat. Phenom. **58**, 325 (1992).
[15] R. Cowan, *The Theory of Atomic Structure and Spectra* (University of California Press, Berkeley, 1981).
[16] P. H. Butler, *Point Group Symmetry Application* (Plenum Press, New York, 1981).
[17] The magnetic moments are calculated by the Hamiltonian H_{mag} and the wave function $|g\rangle=c_n|d^n\rangle+c_{n+1}|d^{n+1}\underline{L}\rangle$. The Hamiltonian H_{mag} is shown as follows: $H_{\mathrm{mag}}=-\mu_{\mathrm{B}}(L_{\mathrm{Ni}}+2S_{\mathrm{Ni}})H_{\mathrm{MF}}$, where L_{Ni} and S_{Ni} denote the orbital and spin angular momentum of the Ni $3d$ shell. The values of c_n and c_{n+1} are estimated by the analysis of the experimental XAS spectra.
[18] T. Mizokawa, A. Fujimori, T. Arima, Y. Tokura, N. Mori, and J. Akimitsu, Phys. Rev. B **52**, 13865 (1995).
[19] T. Uozumi, K. Okada, A. Kotani, R. Zimmermann, P. Steiner, S. Hüfner, Y. Tezuka, and S. Shin, J. Electron Spectrosc. Relat. Phenom. **83**, 9 (1997).
[20] J. Zaanen, G. A. Sawatzky, and J. W. Allen, Phys. Rev. Lett. **55**, 418 (1985).